Metabolism 145 (2023) 155612

Contents lists available at ScienceDirect

Metabolism

journal homepage: www.journals.elsevier.com/metabolism

Increased expression of sodium-glucose cotransporter 2 and *O*-GlcNAcylation in hepatocytes drives non-alcoholic steatohepatitis

Hye Jin Chun [a,b,1], Eun Ran Kim [b,c,1], Minyoung Lee [b,d,1], Da Hyun Choi [a,b], Soo Hyun Kim [b], Eugene Shin [b], Jin-Hong Kim [e], Jin Won Cho [a,f], Dai Hoon Han [g,*], Bong-Soo Cha [b,d,**], Yong-ho Lee [a,b,d,**]

[a] *Interdisciplinary Program of Integrated OMICS for Biomedical Science, Yonsei University, Seoul 03722, Republic of Korea*
[b] *Department of Internal Medicine, Yonsei University College of Medicine, Seoul 03722, Republic of Korea.*
[c] *Division of Endocrine and Kidney Disease Research, Department of Chronic Disease Convergence Research, Korea National Institute of Health, Korea Disease Control and Prevention Agency, Cheongju-si, Chungbuk 28159, Republic of Korea*
[d] *Institute of Endocrine Research, Yonsei University College of Medicine, Seoul 03722, Republic of Korea.*
[e] *Department of Biological Sciences, College of Natural Sciences, Seoul National University, Seoul 08826, Republic of Korea*
[f] *Department of Systems Biology, Glycosylation Network Research Center, Yonsei University, Seoul 03722, Republic of Korea.*
[g] *Department of Surgery, Yonsei University College of Medicine, Seoul 03722, Republic of Korea.*

ARTICLE INFO

Keywords:
Non-alcoholic steatohepatitis
Sodium-glucose transport protein 2
O-linked *N*-acetylglucosamine
Autophagy
Diabetes

ABSTRACT

Aims: Steatosis reducing effects of sodium-glucose cotransporter 2 (SGLT2) inhibitors in non-alcoholic steatohepatitis (NASH) has been consistently reported in humans, but their mechanism remains uncertain. In this study, we examined the expression of SGLT2 in human livers and investigated the crosstalk between SGLT2 inhibition and hepatic glucose uptake, intracellular *O*-GlcNAcylation, and autophagic regulation in NASH.

Materials and methods: Human liver samples obtained from subjects with/without NASH were analyzed. For *in vitro* studies, human normal hepatocytes and hepatoma cells were treated with SGLT2 inhibitor under high-glucose and high-lipid conditions. NASH *in vivo* was induced by a high-fat, −fructose, and -cholesterol Amylin liver NASH (AMLN) diet for 10 weeks followed by an additional 10 weeks with/without SGLT2 inhibitor (empagliflozin 10 mg/kg/day).

Results: Liver samples from subjects with NASH were associated with increased SGLT2 and *O*-GlcNAcylation expression compared with controls. Under NASH condition (*in vitro* condition with high glucose and lipid), intracellular *O*-GlcNAcylation and inflammatory markers were increased in hepatocytes and SGLT2 expression was upregulated; SGLT2 inhibitor treatment blocked these changes by directly reducing hepatocellular glucose uptake. In addition, decreased intracellular *O*-GlcNAcylation by SGLT2 inhibitor promoted autophagic flux through AMPK-TFEB activation. In the AMLN diet-induced NASH mice model, SGLT2 inhibitor alleviated lipid accumulation, inflammation, and fibrosis through autophagy activation related to decreased SGLT2 expression and *O*-GlcNAcylation in the liver.

Abbreviations: SGLT2, sodium-glucose cotransporter 2; NASH, nonalcoholic steatohepatitis; *O*-GlcNAcylation, O-linked β-*N*-acetylglucosamine modification; AMLN, Amylin liver NASH; NAFLD, non-alcoholic fatty liver disease; T2D, type 2 diabetes; *O*-GlcNAc, O-linked β-*N*-acetylglucosamine; H&E, Hematoxylin and eosin; TG, triglyceride; ALT, alanine aminotransferase; AST, aspartate aminotransferase; DMEM, Dulbecco's modified Eagle's medium; FBS, fetal bovine serum; PS, penicillin, and streptomycin; EMPA, empagliflozin; OA, oleic acid; PA, palmitic acid; PBS, phosphate-buffered saline; HG, high glucose; 2-NBDG, 2-(N-(7-Nitrobenz-2-oxa-1,3-diazol-4-yl) Amino)-2-Deoxyglucose; DAPI, 4′,6-diamidino-2-phenylindole; LPS, lipopolysaccharide; TMG, thiamet G; CQ, chloroquine; OGT, *O*-GlcNAc transferase; OGA, *O*-GlcNAcase; GLUT, glucose transporter; CCL2, C-C motif chemokine ligand 2; TNFA, *tumor necrosis factor alpha*; IL1B, interleukin 1 beta; IL6, interleukin 6; MMP3, matrix metallopeptidase 3; ACTA2, actin alpha 2; COL1A1, collagen Type I alpha 1 chain; TFGB, *transforming growth factor beta*; TFEB, transcription factor EB; LC3-Ⅰ/Ⅱ, microtubule-associated protein 1A/1B-light chain; Met, metformin; Leu, leupeptin; p-AMPK, phosphorylated AMP-activated protein kinase; t-AMPK, total AMP-activated protein kinase; AMPKA1, AMP-activated protein kinase alpha 1; AMPKB1, AMP-activated protein kinase beta 1; AMPKG1, AMP-activated protein kinase gamma 1; NS, not significant; O/E, overexpression..

* Correspondence to: D. H. Han, Department of Surgery, Yonsei University College of Medicine, Seoul, Republic of Korea.
** Corresponding authors at: Department of Internal Medicine, Yonsei University College of Medicine, Seoul, Republic of Korea.
E-mail addresses: dhhan@yuhs.ac (D.H. Han), bscha@yuhs.ac (B.-S. Cha), yholee@yuhs.ac (Y.-h. Lee).
[1] Co-first authors.

https://doi.org/10.1016/j.metabol.2023.155612
Received 3 August 2022; Accepted 1 June 2023
Available online 3 June 2023

Conclusions: This study firstly demonstrates increased SGLT2 expression in NASH and secondly reveals the novel effect of SGLT2 inhibition on NASH through autophagy activation mediated by inhibition of hepatocellular glucose uptake and consequently decreased intracellular *O*-GlcNAcylation.

1. Introduction

Over the past three decades, the incidence of non-alcoholic fatty liver disease (NAFLD) has greatly increased, with NAFLD currently the most prevalent and burdensome chronic liver disease worldwide [1], ranging from simple steatosis to non-alcoholic steatohepatitis (NASH). NAFLD is diagnosed by excluding other secondary causes of hepatic steatosis such as alcohol consumption [2]. Recently a term called "metabolic dysfunction-associated fatty liver disease" (MAFLD) was proposed due to the strong link between NAFLD and insulin resistant-related metabolic dysfunction such as type 2 diabetes (T2D) [3,4]. NAFLD is regarded as the liver manifestation of insulin resistance, which is the characteristic pathophysiology of T2D. Hence, antidiabetic drugs were suggested as promising options for treatment of NASH and, in fact, they do confer benefits for NASH [5,6]. Sodium-glucose cotransporter 2 (SGLT2) inhibitors, the newest class of antidiabetic drugs, have received attention for their unexpected and favorable pleiotropic effects on NAFLD [7–9].

However, no drug has been approved by the U.S. Food and Drug Administration for treatment of NASH [5], as its multifactorial etiology and complex pathogenic mechanism hinders development of fully effective drugs. Hepatic autophagy dysfunction is one important feature of NAFLD, causing hepatocellular lipid accumulation, injury, and fibrosis [10]. In the milieu of NAFLD with hepatic insulin resistance, elevated liver glucose concentration may exacerbate impairment of hepatic autophagy [11,12]. Of note, upregulated *O*-linked β-*N*-acetylglucosamine modification (*O*-GlcNAcylation) responsive to increased hepatocellular glucose might be one of potential mechanisms explaining impaired autophagy in NAFLD [13,14]. Based on growing evidence regarding the role of SGLT2 inhibitor as a regulator of autophagic activity in over-nutrition diseases, SGLT2 inhibitor might be an effective candidate for improving autophagy dysregulation caused by glucose-responsive aberrant *O*-GlcNAcylation [15]. In addition, previously observed SGLT2 expression in a hepatocyte cell line [16] raises the possibility of a direct action by SGLT2 inhibitor on hepatic SGLT2 in NASH.

To the best of our knowledge, no previous clinical or experimental study has confirmed SGLT2 expression in NASH and/or studied the effect of SGLT2 inhibitor on NASH in the context of hepatocellular *O*-GlcNAcylation and autophagy. To test our hypothesis, we analyzed human liver samples obtained from biopsy in the current study. We also conducted *in vitro* and *in vivo* studies using a hepatocyte cell line and high-fat, −fructose, and -cholesterol Amylin liver NASH (AMLN) diet-induced NASH mice model, respectively. Finally, we investigated hepatic SGLT2 expression according to NAFLD status and the effect of SGLT2 inhibition on NASH in association with autophagic regulation mediated by hepatocellular *O*-GlcNAcylation.

2. Materials and methods

2.1. Human liver tissue

Human liver biopsy specimens were obtained from control individuals ($n = 15$) without NAFLD and from individuals with simple steatosis ($n = 21$) and NASH ($n = 8$) who underwent hepatectomy or cholecystectomy at the university-affiliated Severance Hospital, Yonsei University College of Medicine (Seoul, South Korea). Pathologic diagnosis of simple steatosis and NASH was determined using steatosis, activity, and fibrosis score [17]. Exclusion criteria included: type 1 diabetes; medical history of organ transplantation; pregnancy; and excessive alcohol intake (> 140 g/week for men and > 70 g/week for women). Liver tissue was formalin-fixed for pathologic examination of NAFLD by a histological scoring system [18]. The remaining tissue was snap-frozen in liquid nitrogen and stored at −80 °C for subsequent gene expression analysis. All participants provided written informed consent and the study was approved by the independent institutional review board of Severance Hospital, Seoul, Korea (4–2014–0674); the study was conducted in adherence to the tenets of the Declaration of Helsinki.

2.2. Animals

Six-week-old male *C57BL/6J* mice were obtained from Japan SLC, Inc. Mice were housed at 23 ± 1 °C with 12-hour light/12-hour dark cycles and were allowed free access to water and standard mouse chow (PicoLab Rodent Diet 20 #5053). After a 1-week acclimation period the mice were randomly assigned to one of three groups according to diet and drug treatment: Group 1, chow-fed mice with vehicle treatment (0.5 % carboxymethyl cellulose [CMC] solution, Sigma-Aldrich) for 20 weeks ($n = 10$); Group 2, AMLN-fed mice with vehicle treatment for 20 weeks ($n = 13$); or Group 3, AMLN-fed mice with vehicle treatment for 10 weeks followed by SGLT2 inhibitor (empagliflozin [EMPA], 10 mg/kg of body weight/day by oral gavage) treatment for 10 weeks ($n = 10$). Regular chow diet was composed of 23.6 % protein, 64.5 % carbohydrate, and 11.9 % fat (% of total kcal) and the AMLN diet (Catalog number D09100301, Research Diets, New Brunswick, NJ, USA) was composed of 20 % protein, 40 % high fat (including 18 % trans-fat), 40 % carbohydrates (% of total kcal), and high cholesterol (2 % by weight). Fructose constituted 22 % of total carbohydrate content by weight. Addition of fructose and trans-fat is a distinct point of this AMLN diet compared to conventional high-fat diet, which is more advantageous to develop NASH animal model [19,20]. Fructose metabolism causes more pronounced lipid accumulation and oxidative stress than glucose metabolism in liver [19], and trans-fat is a superior additive than lard fat to induce NASH animal model due to enhanced lipogenesis and pro-inflammatory process [20,21]. Body weight was monitored weekly. At the end of the study, animals were anesthetized and sacrificed 24 h after the final administration. Blood was collected *via* heart puncture and tissues were harvested. Specimens were snap-frozen in liquid nitrogen and maintained at −80 °C until analysis.

To study the autophagic effect of EMPA, at 21 weeks male *C57BL/6J* mice were divided into two groups and treated every day for one week with oral administration of EMPA (25 mg/kg) or phosphate-buffered saline (PBS). The mice were fed a normal chow diet. In each group, leupeptin (60 mg/kg) or PBS were intraperitoneally injected, and animals were sacrificed 4 h later.

All animal experiments were approved by the Institutional Animal Care and Use Committee of Yonsei University Health System (YUHS-IACUC) regulations and guidelines in accordance with the Animal Protection Act (2008), the Laboratory Animal Act (2008), and the Eighth Edition of the Guide for the Care and Use of Laboratory Animals of NRC (2011).

2.3. Histological analysis

2.3.1. Immunohistochemistry

Human or mouse liver sections were incubated with antibodies against *O*-GlcNAcylation (RL2, 1:100, #MA1–072, Thermo Fisher Scientific) or SGLT2 (1:100, #ab37296, Abcam). Signals were visualized using Vector® DAB peroxidase substrate kit (SK-4100, Vector Lab). Nuclei were counterstained with hematoxylin.

2.3.2. Hematoxylin and eosin (H&E), trichrome, sirius red staining

Liver slides were evaluated for hepatic fat accumulation using a microscope. Human liver sections were stained with H&E or trichrome staining performed using phosphomolybdic acid hydrate (51429-74-4, Junsei), phosphotungstic acid hydrate (12501-23-4, Junsei), acid fuchsin (F8129, Sigma), ponceau BS (B6008, Sigma) and hematoxylin (H3136, Sigma).

In a separate study, sirius red staining of mouse liver was conducted using the Picrosirius Red Stain Kit (24901, Polysciences Inc.).

2.4. Hepatic triglyceride

Liver tissue (30 mg) was homogenized and measured using hepatic triglyceride (TG, ETGA-200, EnzyChrom) following the manufacturer's instructions.

2.5. Blood chemistry assays in in vivo models

Serum levels of insulin were estimated using Morinaga Ultra Sensitive Mouse/Rat Insulin enzyme-linked immunosorbent assay kit (M1104, Morinaga Institute of Biological Science, Yokohama, Japan) according to the manufacturer's instructions. The homeostasis model assessment of and insulin resistance (HOMA-IR) was calculated as (fasting insulin [μIU/mL] × fasting glucose [mg/dL])/405 [22]. For oral glucose tolerance test (OGTT), 4 h-fasted mice were administered glucose at 2 g/kg body weight *via* oral gavage. Insulin tolerance test (ITT) was performed after 4-h fasting using intraperitoneal injection of insulin (0.75 U/kg).

2.6. Non-invasive assessment of hepatic steatosis and fibrosis in human subjects

Hepatic fibrosis was assessed using NAFLD fibrosis score: $-1.675 + 0.037 \times$ age (year) $+ 0.094 \times$ body mass index (kg/m^2) $+ 1.13 \times$ (impaired fasting glucose or diabetes mellitus [yes = 1, no = 0]) $+ 0.99 \times$ AST/ALT ratio $- 0.013 \times$ platelet (10^9/L) $- 0.66 \times$ albumin (g/dL) and fibrosis–4 [FIB–4] index: age (year) × AST (IU/L)/platelet (10^9/L) × ALT$^{1/2}$ (IU/L) [23].

2.7. In vitro cell culture system

2.7.1. Cell culture

Human hepatoma HepG2 and human normal hepatocyte MIHA cells were selected to establish *in vitro* NASH model, as HepG2 and MIHA Cells have been successfully applied to develop lipid accumulation and pro-inflammatory response induced by free fatty acids including oleic acid (OA) and palmitic acid (PA) [10,24–27]. HepG2 or MIHA cells were maintained in Dulbecco's modified Eagle's medium (DMEM, #SH30243.01, Cytiva Hyclone, 25 mM glucose) supplemented with 10 % fetal bovine serum (FBS, #SH30919.03, Cytiva Hyclone), 1 % penicillin, and streptomycin (PS, #SV30010, Cytiva Hyclone). The cells were maintained in an atmosphere of 5 % CO_2 at 37 °C. Detailed information regarding experiments with primary human hepatocytes are described in supplementary materials.

2.7.2. Oil red O staining

HepG2 cells were seeded at a density of 2×10^5 cells/well in a 6-well plate. After 24 h, the cells were incubated with EMPA (10, 25, or 50 μM) for 6 h followed by treatment with oleic acid (1 mM; #O1383, Sigma) only or with EMPA (10, 25, or 50 μM) for 18 h. Oil red O staining was performed. In brief, cells were fixed with 3.7 % formalin for 3 min, followed by rinsing with 60 % isopropanol and staining with Oil red O working solution for 1 h at room temperature. After removing the working solution, the cells were rinsed with distilled water and images were taken using a microscope (Olympus IX73).

2.7.3. In vitro study models

PA (#P9767, Sigma) was dissolved in 1X PBS (#BPB-9121, Tech&Innovation) and 1N Sodium hydroxide (NaOH, #1310-73-2, Georgiachem, Norcross) at a stock concentration of 5 mM. To study hepatocytes under NASH conditions, normal human hepatocyte MIHA cells were seeded at a density of 2×10^5 cells/well in a 6-well plate. The following day, the media was replaced with PA (0.4 mM) or PA plus high glucose (HG, 50 mM) and incubated for 24 h. In this study, high-glucose condition was defined as 50 mM glucose to sufficiently increase intracellular *O*-GlcNAcylation level, considering a dose-dependent relationship between glucose concentration and intracellular *O*-GlcNAcylation level in hepatocyte [28,29]. Cells were harvested to conduct immunoblot assays. To study the overexpression of SGLT2, MIHA cells were seeded at a density of 5×10^5 cells/well in a 6-well plate and cultured overnight. The following day, the media was replaced with fresh DMEM with glucose (25 mM) without penicillin or streptomycin. The recombinant plasmid p3xFlag-SGLT2 (3 μg) was transfected into MIHA cells by mixing with Lipofectamine™3000 reagent (#L3000-015, Invitrogen) in Opti-MEM media (#31985070, Gibco) and was further cultured for 24 h. To assess the effects of EMPA in a PA + HG model, HepG2 cells were seeded at a density of 2×10^5 cells/well in a 6-well plate and incubated overnight with PA (0.4 mM) + HG (50 mM glucose) or PA + HG + EMPA (50 μM) for 24 h. To assess inflammation in the NASH *in vitro* model, MIHA cells were cultured in DMEM with a low amount of glucose (5.5 mM). Following overnight culturing, cells were treated with PA (0.4 mM) + lipopolysaccharide (LPS, 0.1 μg/mL), PA + LPS + EMPA (50 μM) in DMEM with glucose (11.5 mM), or DMEM with glucose (25 mM) for 24 h. To study *O*-GlcNAcylation-autophagy regulation, HepG2 cells were incubated with an OGA inhibitor, thiamet G (TMG, 10 μM, #SML0244, Sigma), EMPA (25 μM), or chloroquine (CQ, 10 μM; #C-6628, Sigma) for 4 h either separately or together. In a separate study, HepG2 cells in DMEM (with 25 mM glucose) were treated with TMG (10 μM), EMPA (50 μM), or torin (200 nM) for 6 h. To examine various possible outcomes, HepG2 cells were incubated with EMPA (25 μM) for various periods of time (1, 2, 4, or 16 h) and metformin (2 mM) for 16 h. The glucose concentration in the culture media was 25 mM unless specified otherwise. After each study, cells were harvested for mRNA or protein analysis.

To study the inhibition of SGLT2, MIHA cells were seeded at a density of 5×10^5 cells/well in a 6-well plate and cultured overnight. The following day, control siRNA-fluorescein conjugate (#sc-36869, Santa Cruz Biotechnology) or SGLT2 siRNA (#sc-106547, Santa Cruz Biotechnology) was transfected into MIHA cells by mixing with siRNA transfection reagent (#sc-29528, Santa Cruz Biotechnology) and was further cultured for 6 h. The media was replaced with fresh DMEM with glucose (25 mM) without penicillin or streptomycin and siRNA transfection was repeated.

To study the uptake of 2-(N-(7-Nitrobenz-2-oxa-1,3-diazol-4-yl) Amino)-2-Deoxyglucose (2-NBDG, #N13195, Thermo Fisher Scientific), HepG2 cells were cultured overnight. The culture media was removed, followed by a rinse with 1X PBS, repeated × 3. The cells were incubated for 2 h with DMEM (no glucose) before treatment with EMPA (30, 100 μM) and 2-NBDG (200 μM). After incubation for 1 h, cells were fixed and stained using 4′,6-diamidino-2-phenylindole (DAPI). Fluorescence was observed and images were taken using a microscope (Olympus IX73). The intensity of the fluorescence was analyzed using ImageJ software (National Institutes of Health, USA).

To assess *O*-GlcNAcylation in the NASH *in vitro* model, MIHA cells were cultured in DMEM. Following overnight culturing, cells were treated with PA (0.4 mM) + LPS (0.1 μg/mL) and TMG (10 μM) in DMEM with high glucose (50 mM) for 24 h.

To study the increase of *O*-GlcNAcylation, MIHA cells were seeded at a density of 5×10^5 cells/well in a 6-well plate and cultured overnight. The following day, the media was replaced with fresh DMEM with glucose (25 mM) without penicillin or streptomycin. The recombinant plasmid p3xFlag-*O*-GlcNAc transferase (OGT, 3 μg) was transfected into

MIHA cells by mixing with Lipofectamine™3000 reagent (#L3000-015, Invitrogen) in Opti-MEM media (#31985070, Gibco) and was further cultured for 24 h.

To study *O*-GlcNAcylation-autophagy regulation, HepG2 cells were incubated with TMG (10 μM, #SML0244, Sigma), EMPA (25 μM), or CQ (10 μM; #C-6628, Sigma) for 4 h either separately or together. In a separate study, HepG2 cells in DMEM (with 25 mM glucose) were treated with TMG (10 μM), EMPA (50 μM), or torin (200 nM) for 6 h. To examine various possible outcomes, HepG2 cells were incubated with EMPA (25 μM) for various periods of time (1, 2, 4, or 16 h) and metformin (2 mM) for 16 h.

To evaluate SGLT2-*O*-GlcNAcylation-autophagy regulation, control siRNA-fluorescein conjugate or SGLT2 siRNA was transfected into MIHA cells by mixing with siRNA transfection reagent and was further cultured for 6 h. The media was replaced with fresh DMEM with glucose (25 mM) without penicillin or streptomycin and siRNA transfection was repeated and further cultured for 6 h. Following the culturing, cells were treated with PA (0.4 mM), TMG (10 μM) in DMEM with high glucose (50 mM) for 24 h.

2.8. Immunoblot analysis and antibodies

Immunoblot assays were performed as previously described [10]. The following antibodies were used: *O*-GlcNAcylation (RL2, #MA1-072, Thermo Fisher Scientific); hSGLT2 (#ab37296, Abcam); mSGLT2 (#85626, Abcam); GLUT1 (#MABS132, Sigma); GLUT2 (#20436-1-AP, Proteintech); OGT (#O6264, Sigma); *O*-GlcNAcase (OGA, #ab124807, Abcam); p-AMPK (#2535S, Cell signaling); t-AMPK (#2603, Cell signaling); β-actin (#A5441, Sigma); transcription factor EB (TFEB, #A303-673A, Bethyl Laboratories); Histone-H3 (#06-599, Sigma); and LC3-Ⅰ/Ⅱ (#L7543, Sigma).

2.9. Quantitative RT-PCR analysis

Total RNA was prepared from cultured cells or tissues using TRIzol® reagent (MRC, TR 118). RNA (1 μg) was then subjected to reverse transcription with random-hexamer primers and a High Capacity cDNA Reverse Transcription Kit (#4368813, Applied Biosystems). The quantitative PCR was performed using SYBR® Green PCR Master Mix (#4367659, Applied Biosystems). The sequences of the primers are listed as supplementary material.

2.10. Statistics

In vitro and *in vivo* data are presented as means ± standard errors of the mean (SEM). In analyses of *in vitro* and *in vivo* data, statistical significance among the groups was derived using a one-way analysis of variance (ANOVA) test followed by hoc test, student-*t*-test, Mann-Whitney *U* test, or Wilcoxon rank sum test. Human data are presented as mean and standard deviation values for normally distributed continuous variables or median and interquartile range values for non-normally distributed continuous variables. Data of categorical variables are presented as numbers with percentages (%). The difference among normal, simple steatosis, and NASH groups was analyzed using ANOVA for continuous variables with normal distribution and the Jonckheere-Terpstra test for continuous variables with non-normal distribution. The difference in categorical variables among normal, simple steatosis, and NASH groups was assessed using the chi-squared test or Fisher's exact test according to expected frequency. Correlations between the relative hepatic SGLT2 expression level, clinical variables, and the expression level of genes related to inflammation, fibrosis, and autophagy, were evaluated using Pearson's correlation coefficient. Statistical analysis was conducted using GraphPad Prism. Statistical significance was defined as $P < 0.05$.

3. Results

3.1. Human NASH demonstrates increased SGLT2 expression and O-GlcNAcylation in liver

We investigated liver histopathology and hepatic SGLT2 expression, *O*-GlcNAcylation, and other relevant genes expression levels in individuals of three groups (normal, simple steatosis, and NASH) with clinical characteristics presented in Supplementary Table 1. Individuals in the NASH group showed a higher prevalence of T2D ($p = 0.001$) and had a higher level of body mass index and fasting glucose (all $p < 0.05$) than those in the normal and steatosis groups. Serum liver enzymes and γ-glutamyl transferase levels were significantly higher in the NASH group than in the others (all $p < 0.05$).

H&E or trichrome staining was performed on liver sections to determine fat accumulation and collagen deposition, which are important characteristics of NASH. NASH samples had large fat droplets and fibrosis compared to controls (Fig. 1A). Then, the mRNA expression levels of SGLT2, genes known to be involved in *O*-GlcNAcylation (*OGT* and *OGA*), and glucose transporter (GLUT) genes (*GLUT1* and *GLUT2*), were assessed. Although there were no differences in the gene expression levels of *GLUT1*, *GLUT2*, *OGT*, and *OGA* among the different stages of NAFLD spectrum (Fig. 1B), the expression of SGLT2 and *O*-GlcNAcylation was clearly increased in simple steatosis and NASH compared to normal livers (Fig. 1C). In addition, hepatic *SGLT2* mRNA expression was significantly increased in the NASH group (Fig. 1D). These results indicate that NASH pathology is significantly associated with high levels of SGLT2 and *O*-GlcNAcylation.

Moreover, among various clinic-laboratory parameters, relative hepatic *SGLT2* mRNA expression levels showed a significant positive correlation with the degree of hepatic fibrosis determined using NAFLD fibrosis score ($p = 0.039$) and FIB–4 ($p = 0.041$, Table 1). Furthermore, hepatic expression of genes related to inflammation (IL6), fibrosis (ACTA2) significantly correlated with SGLT2 expression, suggesting a pathophysiologic role of increased hepatic SGLT2 expression in pro-inflammatory/pro-fibrogenic process in NASH (Fig. 1E).

3.2. Upregulated SGLT2 expression in association with intracellular O-GlcNAcylation in hepatocytes under NASH conditions and impact of O-GlcNAcylation in other cell types

To assess whether upregulated SGLT2 is related to *O*-GlcNAcylation levels in NASH, *O*-GlcNAc, SGLT2, GLUT1, and GLUT2 protein levels were studied using western blotting. MIHA cells incubated with PA + HG were used to mimic NASH conditions. *O*-GlcNAcylation levels increased with exposure to PA + HG. Increased *O*-GlcNAcylation was accompanied by increased SGLT2 expression but with lower GLUT1 and GLUT2 expression. This observation was stronger in the PA + HG group compared to the PA-only group (Fig. 2A). Consistently, *SGLT2* mRNA expression was increased in the PA-only group and this increase was even greater with PA + HG incubation. Notably, *O*-GlcNAcylation was also significantly increased by incubation with PA + HG (Fig. 2A), suggesting that NASH increases hepatic levels of SGLT2 and *O*-GlcNAcylation. The expression level of GLUT2 was reduced, and there was no change in GLUT1 (Fig. 2A and B). Furthermore, the expressions of *OGT* and *OGA* genes, which regulate *O*-GlcNAcylation, were changed in a yin-yang pattern, with reduced *OGT* expression and increased *OGA* expression, possibly indicating a feedback loop. To assess whether high SGLT2 levels upregulate *O*-GlcNAcylation in NASH liver, SGLT2 was overexpressed in human hepatocytes and protein levels were evaluated. As expected, *O*-GlcNAcylation and gene expression associated with inflammation or fibrosis were increased with SGLT2 expression (Fig. 2C, Fig. S1A and B). Importantly, the expressions of other glucose transporters tended to be decreased. OGA was markedly increased, and OGT was slightly decreased. These data indicate that *O*-GlcNAcylation may be regulated by hepatic SGLT2 signals in NASH.

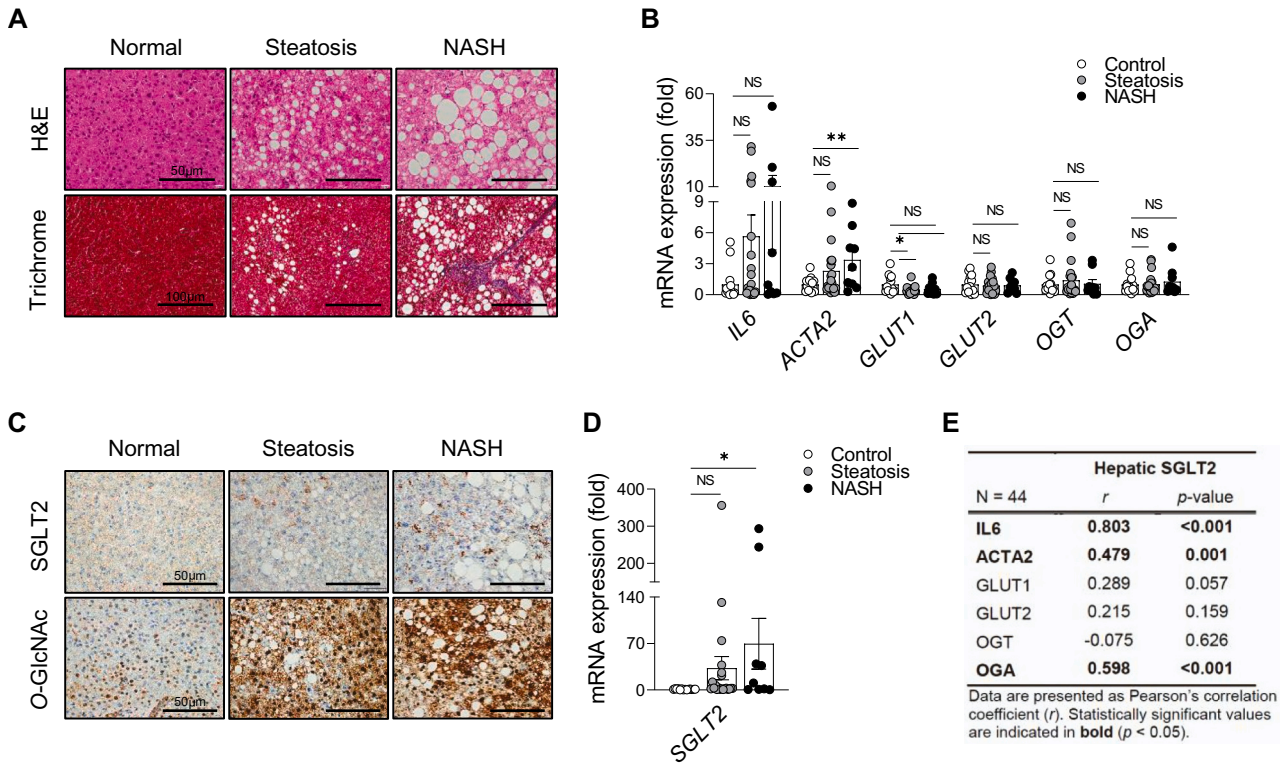

Fig. 1. Non-alcoholic steatohepatitis (NASH) increases SGLT2 and *O*-GlcNAcylation expression levels in the human liver. (A) Representative staining for fat and collagen in healthy human liver and human liver with simple steatosis and NASH. (B) Real-time qPCR for mRNA expression levels of *IL6*, *ACTA2*, *GLUT1*, *GLUT2*, *OGT*, and *OGA*. (C) Immunohistochemistry of SGLT2 and *O*-GlcNAcylation in the liver. (D) Real-time qPCR for mRNA expression levels of *SGLT2*. (E) Correlations between the relative hepatic mRNA expression levels of *SGLT2* and other genes. Data are expressed as mean ± SEM. *$P < 0.05$ by Student's *t*-test.

Table 1
Correlation analyses between the relative hepatic SGLT2 mRNA expression level and clinic-laboratory parameters in study participants.

	Hepatic SGLT2 expression	
$N = 44$	*r*	*p*-value
Age (years)	0.210	0.170
BMI (kg/m^2)	0.153	0.321
Fasting glucose (mg/dL)	0.145	0.349
Total cholesterol (mg/dL)	−0.245	0.118
Triglyceride (mg/dL)	−0.218	0.417
HDL-C (mg/dL)	−0.488	0.065
LDL-C (mg/dL)	−0.369	0.214
AST (IU/L)	0.037	0.814
ALT (IU/L)	−0.056	0.722
AST/ALT ratio	0.038	0.810
γ-glutamyl transferase (IU/L)	−0.003	0.990
Total bilirubin (mg/dL)	0.201	0.191
NAFLD fibrosis score	**0.320**	**0.039**
FIB–4	**0.314**	**0.041**

Data are presented as Pearson's correlation coefficient (*r*). Statistically significant values are indicated in **bold** ($p < 0.05$).
ALT, alanine aminotransferase; AST, aspartate aminotransferase; BMI, body mass index; FIB–4, fibrosis–4; HDL—C, high-density lipoprotein-cholesterol; LDL-C, low-density lipoprotein-cholesterol; NAFLD, non-alcoholic fatty liver disease; SGLT2, sodium-glucose cotransporter 2.

Furthermore, SGLT2 levels negatively correlated with the phosphorylation of AMPK, suggesting that metabolic disorders in NASH may be related to high levels of SGLT2 in the liver. To evaluate the role of SGLT2 in NASH gene expression, inflammation and fibrosis markers were measured. The results show that *CCL2*, *TNFA*, *IL1B*, *MMP3*, *ACTA2*, and *TGFB* levels were substantially increased (Fig. 2D). Similarly, direct overexpression of *OGT* or TMG treatment resulted in increased cellular levels of *O*-GlcNAcylation, gene expression associated with inflammation, and fibrosis in hepatocytes (Fig. 2E and F). Consistent with these findings, TMG also increased intracellular *O*-GlcNAcylation and inflammation/fibrosis related gene expressions in both hepatocyte cell lines including MIHA (Fig. 2G-H) and primary human hepatocytes (Fig. S2A and B), as well as in hepatic stellate cells and macrophages (Fig. S3A-D). Furthermore, SGLT2-*O*-GlcNAcylation signaling disturbed hepatic insulin signaling pathways and induced the expression of lipogenic genes, which were ameliorated by the SGLT2 inhibitor, EMPA treatment (Fig. S4A-D). Therefore, SGLT2 in hepatocytes may be involved in inflammation and fibrosis gene regulation, perhaps mediated by *O*-GlcNAcylation and *O*-GlcNAcylation can affect NASH phenotypes in other cell types.

3.3. Decreased expression of SGLT2 attenuates O-GlcNAcylation-mediated inflammation in hepatocytes under NASH conditions

To assess whether decrease in SGLT2 levels downregulates *O*-GlcNAcylation in NASH liver, expression levels of SGLT2 were inhibited in human hepatocytes and protein levels were evaluated. Reduced SGLT2 expression levels in the NASH mimic cell system reduced *O*-GlcNAcylation levels, followed by a reduction in gene expression of inflammation and fibrosis to normal levels (Fig. 3A and B). In the *in vitro* system of the NASH condition (PA + HG), *O*-GlcNAcylation was highly increased, and these levels were suppressed by EMPA (Fig. 3C), indicating that SGLT2 may induce *O*-GlcNAcylation in NASH. The induction of SGLT2 protein levels in NASH was not changed by EMPA treatment. Similarly, expressions of glucose transporters GLUT1 and GLUT2, were not altered by EMPA. To mimic fatty liver, HepG2 cells were incubated with oleic acid (OA). Intracellular triglyceride (TG) levels were significantly increased and were ameliorated by EMPA treatment (Fig. 3D). In addition, gene expression levels of hepatic inflammation (*CCL2*, *IL6*, and *TNFA*) and fibrosis (*ACTA2*, *COL1A1*, and *TGFB*), which were induced by treatment with PA + LPS or PA + HG + LPS, were reduced by EMPA

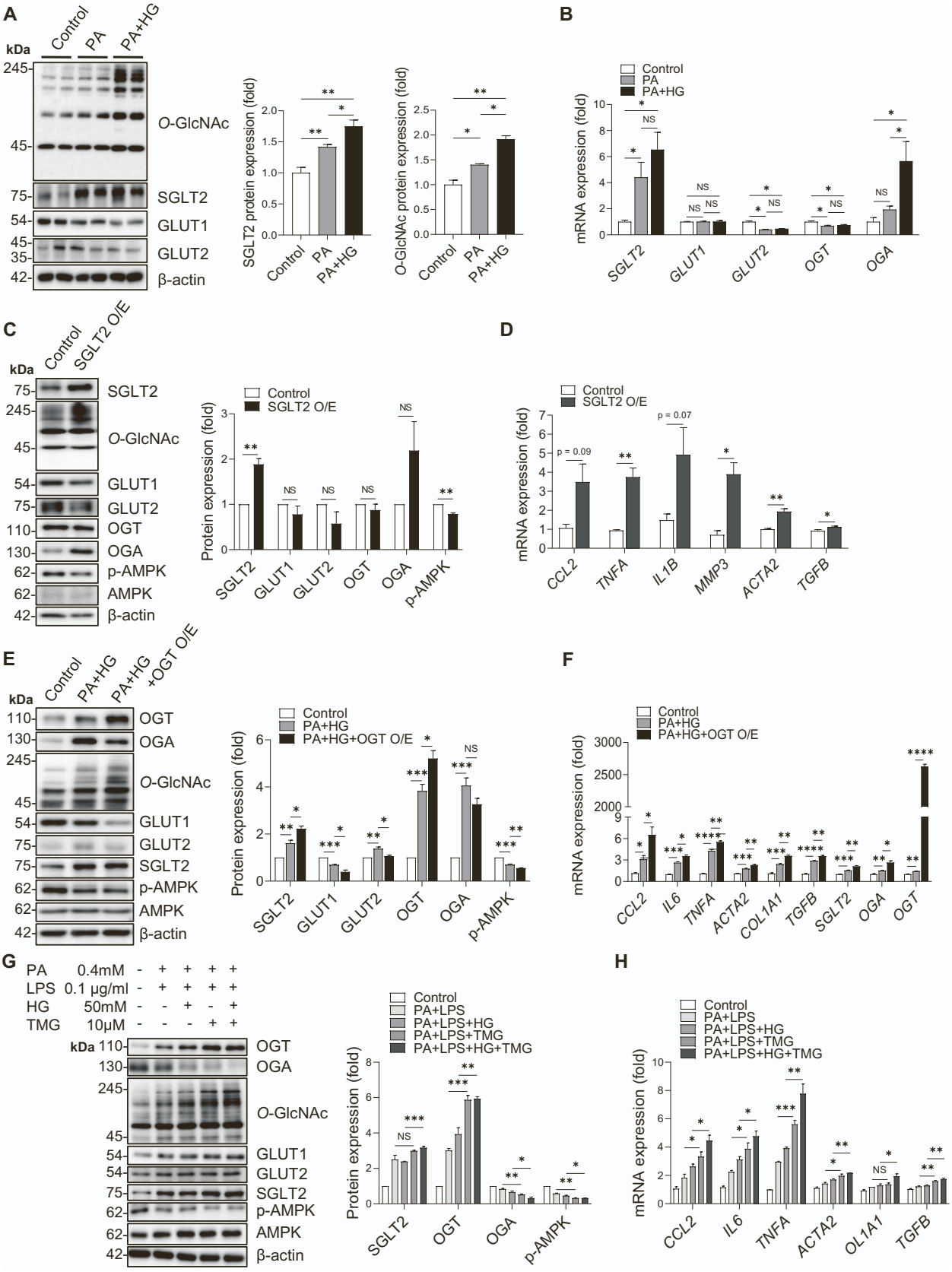

(caption on next page)

Fig. 2. Upregulated hepatic SGLT2 or OGT expression levels and *O*-GlcNAcylation in an *in vitro* NASH model. MIHA cells have been incubated with palmitic acid (PA) or PA plus high glucose (HG, 50 mM) for 24 h, along with controls, and analyzed for (A) immunoblots of *O*-GlcNAcylation, SGLT2, GLUT1, and GLUT2, and β-actin. (B) Real-time qPCR for mRNA expression levels of *SGLT2*, *GLUT1*, *GLUT2*, *OGT*, and *OGA*. (C) *SGLT2* plasmid has been transfected into MIHA cells and cultured for 24 h, and protein expression levels of SGLT2, *O*-GlcNAcylation, GLUT1, GLUT2, OGT, OGA, p-AMPK, total AMPK, and β-actin are measured. (D) Expression levels of genes associated with inflammation and fibrosis (*CCL2*, *TNFA*, *IL1B*, *MMP3*, *ACTA2*, and *TGFB*). (E) *OGT* plasmid has been transfected into MIHA cells and cultured 24 h, and protein expression levels of OGT, OGA, *O*-GlcNAcylation, GLUT1, GLUT2, SGLT2, p-AMPK, total AMPK, and β-actin are measured. (F) Real-time qPCR for mRNA expression levels of genes associated with inflammation, fibrosis, *SGLT2*, *OGA*, and *OGT*. (G) TMG has been treated to MIHA cells with PA, LPS and HG followed by measured protein expression levels of OGT, OGA, *O*-GlcNAcylation, GLUT1, GLUT2, SGLT2, p-AMPK, total AMPK, and β-actin. (H) Real-time qPCR for mRNA expression levels of genes associated with inflammation and fibrosis. Data are expressed as mean ± SEM (n = 3–4 per group). *$P < 0.05$, **$P < 0.01$ by Student's *t*-test. CCL2, C—C motif chemokine ligand 2; IL6, interleukin 6; TNFA, tumor necrosis factor alpha; IL1B, interleukin 1 beta; MMP3, matrix metallopeptidase 3; ACTA2, actin alpha 2; COL1A1, collagen type I alpha 1 chain; TGFB, transforming growth factor beta; TMG, thiamet G; LPS, lipopolysaccharide; p-AMPK, phosphorylated AMP-activated protein kinase; t-AMPK, total AMP-activated protein kinase; NS, not significant; O/E, overexpression.

treatment (Fig. 3E). To demonstrate whether beneficial effects of SGLT2 inhibition are mediated by *O*-GlcNAcylation reduction, TMG were treated, showing that the improvement in NASH phenotypes by either EMPA or SGLT2 knockdown were abrogated with TMG treatment (Fig. 3F-I). These results were consistently reproduced in primary human hepatocytes (Fig. S5A and B). In addition, effects of EMPA on lipid accumulation were diminished with TMG in primary human hepatocytes (Fig. S5C). Therefore, NASH development may occur through the SGLT2-*O*-GlcNAcylation pathway.

3.4. SGLT2 inhibitor induces autophagic flux through AMPK-TFEB activation via reduction of intracellular O-GlcNAcylation

To assess whether SGLT2 is responsible for glucose uptake in hepatocytes, 2-NBDG, a fluorescent glucose analog, was used. Under mild fasting conditions (no glucose), 2-NBDG uptake was increased and inhibited by EMPA, an SGLT2 inhibitor (Fig. 4A), indicating that hepatic SGLT2 transports glucose into cells. In line with that decrease in intracellular glucose levels can activate AMPK [30], we confirmed that EMPA stimulated the phosphorylation of AMPK at similar levels of metformin treatment (Fig. 4B). We assessed the role of SGLT2-*O*-GlcNAcylation-AMPK signaling in hepatocytes. In an *in vitro* NASH model, PA + HG significantly reduced mRNA expression levels of AMPK subunits (Fig. 4C). Interestingly, enhancement of *O*-GlcNAcylation by overexpression of *OGT* or TMG (10 μM) treatment under PA + HG conditions further reduced the gene expression levels of AMPKα, β, and γ subunits (Fig. 4C and D). Consistently, these expression patterns were reversed by SGLT2 inhibition using siRNAs or EMPA treatment (Fig. 4C and D).

To further identify SGLT2 pathways in hepatocytes, we examined whether autophagy is a downstream mediator of hepatic SGLT2-*O*-GlcNAcylation signaling by monitoring autophagy flux. HepG2 cells with EMPA treatment significantly increased the LC3 net flux and this effect was blunted with TMG, which increased *O*-GlcNAcylation (Fig. 4E). Along with LC3 flux, we sought to verify whether the pro-autophagic TFEB is involved in this regulation [10]. Similar to torin, an mTOR inhibitor, EMPA activated TFEB with lowered *O*-GlcNAcylation and this observation was reversed by TMG treatment (Fig. 4F).

We also examined downstream mediators of SGLT2 and *O*-GlcNAcylation. Inhibition of *SGLT2* function or expression significantly increased p-AMPK and TFEB expression (Fig. 4G and Fig. S6A). On the other hand, inhibition of autophagy flux by CQ treatment significantly blocked beneficial effects of EMPA or si*SGLT2* on inflammation and fibrosis (Fig. 4H and Fig. S6B). Consistently, these EMPA effects were reproduced in primary human hepatocytes (Fig. S5A and B).

To further demonstrate whether AMPK activation is required for the therapeutic effects of EMPA in hepatocytes, an AMPK inhibitor, compound C, were treated. Compared to the treatment with EMPA alone, co-treatment of EMPA and compound C diminished p-AMPK and TFEB with increase in *O*-GlcNAcylation levels (Fig. S7A) and reversed improved inflammation and fibrosis by EMPA in hepatocytes (Fig. S7B). Therefore, it is plausible that SGLT2-*O*-GlcNAcylation signals may be further mediated through autophagy *via* AMPK and TFEB regulation.

3.5. SGLT2 inhibitor ameliorates NASH phenotypes in amylin diet-induced NASH mice model

To evaluate whether inhibition of SGLT2 function ameliorates NASH progression, a NASH diet mouse model was developed (Fig. 5A). In the EMPA group, body weight was significantly lower than the AMLN group after EMPA administration was initiated at 10th weeks (Fig. 5B). Characteristic features including parameters related to glucose homeostasis according to AMLN diet and EMPA administration at 20th weeks are summarized in Supplementary Table 2. The AMLN group exhibited a significant increase in body weight, liver weight, and liver to body weight ratio compared with the chow group. EMPA administration in the AMLN-fed mice significantly reduced body weight ($p = 0.022$) and numerically decreased liver weight and liver to body weight ratio without statistical significance compared to the vehicle-treated AMLN-fed mice. The levels of fasting serum insulin, HOMA-IR, and area under the curves (AUC) of OGTT and ITT were also significantly higher in the vehicle-treated AMLN-fed mice than in the chow-fed mice (all $p < 0.05$). EMPA treatment significantly attenuated increase in fasting serum insulin, HOMA-IR, and AUC of OGTT in the AMLN-fed mice (all $p < 0.05$). Histological analysis of liver showed severe fat accumulation and collagen deposition with the AMLN diet and these NASH characteristics were ameliorated with EMPA treatment (Fig. 5C). Consistently, the increase in hepatic TG levels with the AMLN diet was significantly reduced with EMPA (Fig. 5D). To further assess the effect of EMPA on NASH, expression levels of genes involved in inflammation and fibrosis were measured. Expression of *Il1b*, *Il6*, *Mcp1*, *Tnfa*, *Acta2*, *Col1a1*, and *Tgfb* genes were significantly suppressed by EMPA except for *Col1a1* (Fig. 5E). These data suggest that inhibition of SGLT2 function improves the pathological phenotype of NASH.

3.6. SGLT2 inhibitor enhances autophagy function by decreasing O-GlcNAcylation in the liver of amylin diet-induced NASH mice model

The protein expression levels of SGLT2, *O*-GlcNAc, nuclear TFEB, and LC3-Ⅰ/Ⅱ were measured to evaluate whether disturbance of SGLT2 affects the *O*-GlcNAcylation and autophagy signals in a NASH animal model. As shown previously in the human NASH liver (Fig. 1C), SGLT2 levels and *O*-GlcNAcylation were upregulated in the AMLN diet-fed NASH livers of mice (Fig. 6A). These were reversed in the EMPA group. Interestingly, reduced SGLT2 and *O*-GlcNAcylation by EMPA treatment enhanced autophagy by increasing p-AMPK and nuclear TFEB (Fig. S8A and Fig. 6A and B). Gene expression levels of *Sglt2* that were increased by the AMLN diet were reduced in the EMPA group. *Glut1* and *Glut2* mRNA levels were reduced. Enzymes for regulation of *O*-GlcNAcylation, *Ogt* and *Oga*, were upregulated in the AMLN group and their levels in the EMPA group were comparable to controls. Lastly, there were no changes in any group for *Tfeb* (Fig. 6C). This may be because TFEB protein levels affect or function through its translocation into the nucleus rather than through gene expression. Consistent with *in vitro* data, suppression of SGLT2 function with EMPA increased the expression levels of AMPKα, β, and γ subunits (Fig. 6D). In an independent study, EMPA induced autophagic flux in the mouse liver (Fig. S8B),

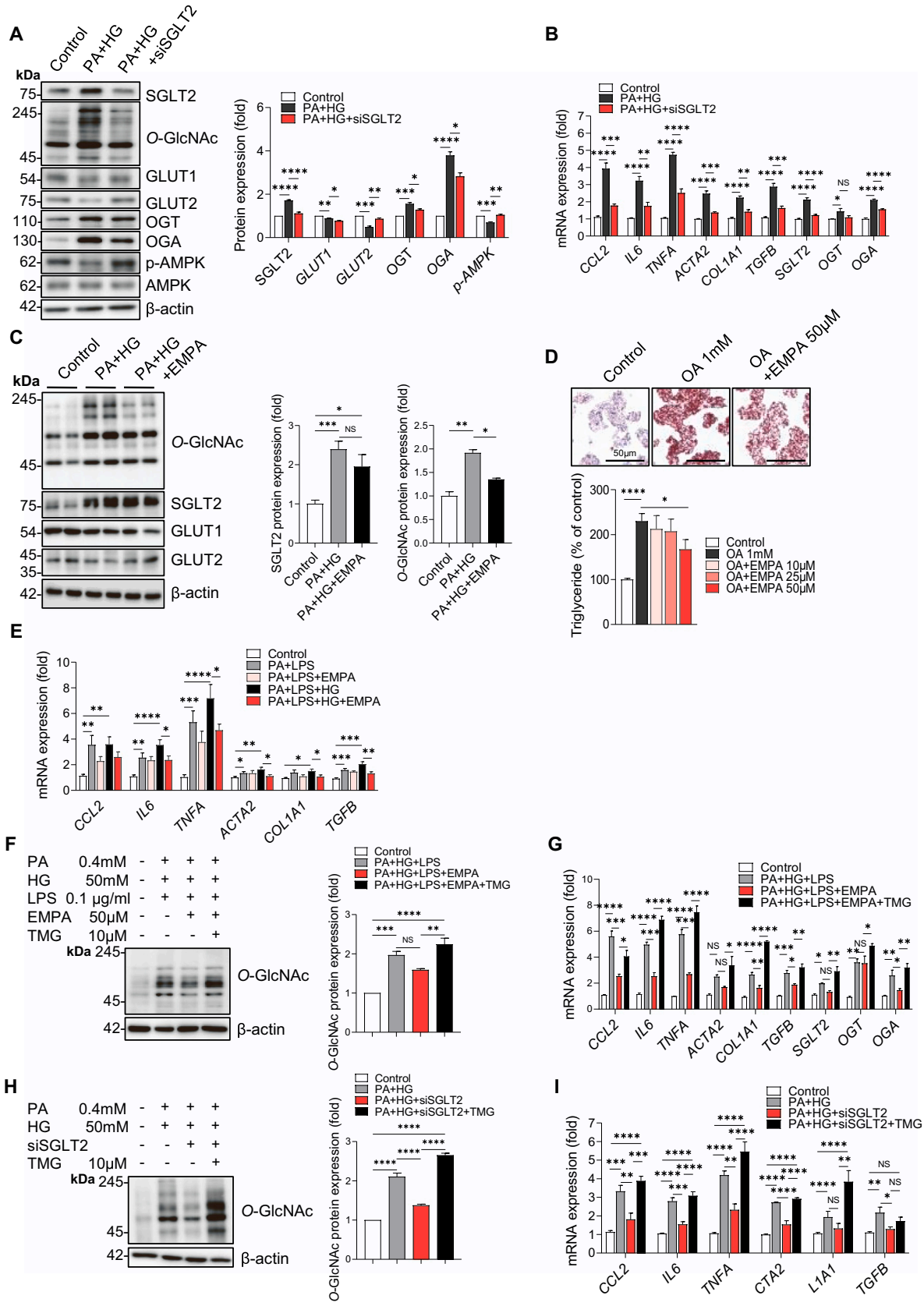

(caption on next page)

Fig. 3. Inhibition of hepatic SGLT2 function reduces expression of *O*-GlcNAcylation and genes associated with inflammation and fibrosis in an *in vitro* NASH model. (A) si*SGLT2* plasmid has been transfected into MIHA cells, and expression levels of proteins and (B) genes are measured. (C) Immunoblot analysis of *O*-GlcNAcylation, SGLT2, GLUT1, GLUT2, and β-actin from the lysate of HepG2 cells that were incubated in a control medium (25 mM), PA (0.4 mM) + HG (50 mM), or PA (0.4 mM) + HG (50 mM) + EMPA (50 μM) for 24 h. (D) Triglyceride contents and Oil red O staining of HepG2 cells with a normal incubation medium, oleic acid (OA, 1 mM), OA (1 mM) + EMPA (10, 25, or 50 μM). (E) Real-time qPCR for mRNA expression of *CCL2*, *IL6*, *TNFA*, *ACTA2*, *COL1A1*, and *TGFB* from lysates of MIHA cells incubated with a control medium (11.5 mM glucose), PA (0.4 mM) + LPS (0.1 μg/mL) in the absence or presence of EMPA (50 μM) in DMEM with glucose (11.5 or 25 mM) for 24 h. (F) EMPA (50 μM) or TMG (10 μM) has been treated to MIHA cells with PA (0.4 mM), LPS (0.1 μg/mL), and HG (50 mM) and *O*-GlcNAcylation levels were measured. (G) Real-time qPCR for mRNA expression levels of genes associated with inflammation, fibrosis, *SGLT2, OGA*, and *OGT*. (H) si*SGLT2* or si*SGLT2* + TMG (10 μM) has been treated to MIHA cells with PA (0.4 mM) and HG (50 mM). (I) Real-time qPCR for mRNA expression levels of genes associated with inflammation and fibrosis. Data are expressed as mean ± SEM (n = 4–20 per group); *$P < 0.05$, **$P < 0.01$, ***$P < 0.001$, ****$P < 0.0001$ by Student's *t*-test. p-AMPK, phosphorylated AMP-activated protein kinase; t-AMPK, total AMP-activated protein kinase; EMPA, empagliflozin; PA, palmitic acid; HG, high glucose; OA, oleic acid; LPS, lipopolysaccharides; NS, not significant. (For interpretation of the references to colour in this figure legend, the reader is referred to the web version of this article.)

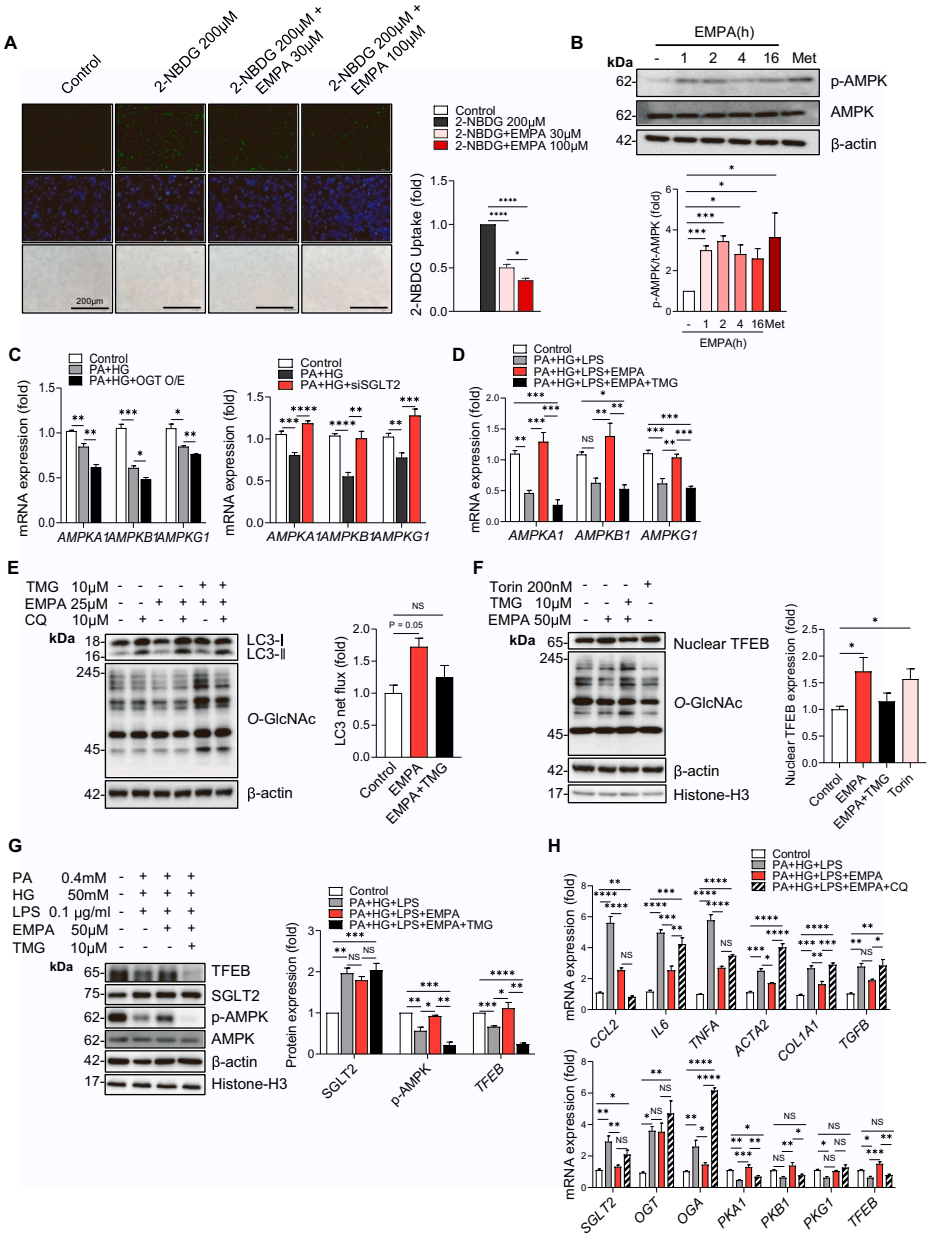

Fig. 4. The SGLT2 inhibitor leads to autophagic flux and nuclear transcription factor EB (TFEB). (A) HepG2 cells have been incubated in a glucose-free medium for 1 h followed by the addition of 2-NBDG in normal glucose media in the absence or presence of EMPA (30 or 100 μM), and fluorescent images were acquired. (B) Phosphorylated AMPK induction with EMPA (25 μM) treatment timely (1, 2, 4, or 16 h) or metformin (2 mM) for 16 h. (C) *OGT* O/E or si*SGLT2* has been transfected to MIHA cells, and (D) EMPA (50 μM) or EMPA + TMG (10 μM) with PA (0.4 mM) + HG (50 mM) + LPS (0.1 μg/mL) has been treated, followed by measuring expression levels of genes (*AMPKA1*, *AMPKB1*, and *AMPKG1*). (E) Immunoblot/densitometric analysis of LC3-Ⅰ/Ⅱ, *O*-GlcNAcylation, and β-actin in HepG2 cell lysate incubated with EMPA (25 μM), TMG (10 μM) + EMPA for 24 h, or with addition of CQ (10 μM) for the last 4 h. (F) Immunoblot/densitometric analysis of TFEB normalized to Histone-H3 and *O*-GlcNAcylation in HepG2 cell lysate incubated with EMPA (50 μM), EMPA (50 μM) + TMG (10 μM) for 24 h, or Torin (200 nM) for 6 h. (G) Protein expression of SGLT2, p-AMPK, and TFEB and (H) mRNA expression of *CCL2*, *IL6, TNFA, ACTA2*, *COL1A1*, *TGFB*, *SGLT2*, *OGT*, *OGA*, *AMPKA1*, *AMPKB1*, *AMPKG1*, and *TFEB* from lysates of MIHA cells incubated with a medium of PA + HG + LPS in the absence or presence of EMPA (50 μM) and with TMG (10 μM) for 24 h or CQ (10 μM) for the last 4 h. Data are expressed as mean ± SEM (n = 3 per group); *$P <$ 0.05 by Student's *t*-test. Met, metformin; O/E, overexpression; TMG, thiamet-G; CQ, chloroquine; LC3-Ⅰ/ Ⅱ, microtubule-associated protein 1A/1B-light chain 3; p-AMPK, phosphorylated AMP-activated protein kinase; t-AMPK, total AMP-activated protein kinase; AMPKA1, AMP-activated protein kinase alpha 1; AMPKB1, AMP-activated protein kinase beta 1; AMPKG1, AMP-activated protein kinase gamma 1; NS, not significant.

thereby promoting autophagy. In summary, we confirmed our findings, namely that SGLT2 is induced in NASH and mediates NASH pathology through *O*-GlcNAcylation-mediated autophagy signaling transduction, using an animal model (Fig. 6E).

4. Discussion

This study demonstrates that hepatic SGLT2 expression is significantly upregulated under NASH conditions, implying an expanding role for the SGLT2 protein as a hepatic glucose transporter in NASH compared to normal liver, as well as a novel mechanism whereby SGLT2

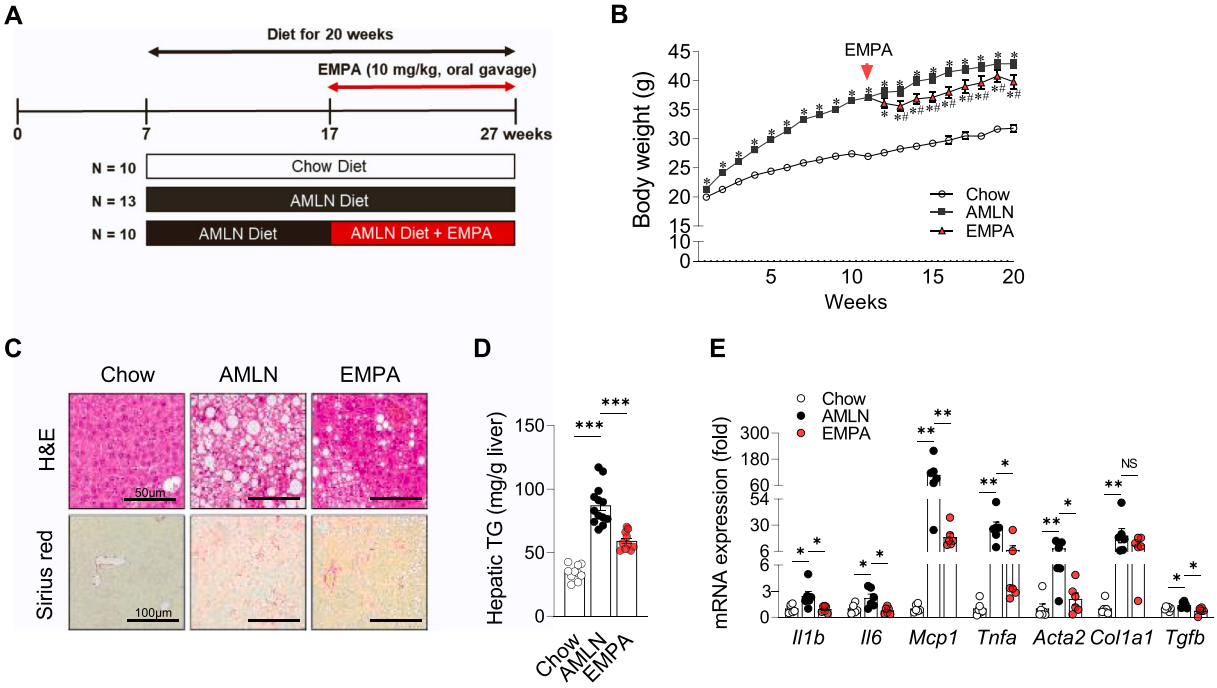

Fig. 5. SGLT2 inhibitor improves NASH in an amylin liver non-alcoholic steatohepatitis (AMLN) diet mice model. (A) Schematic diagram of experimental procedure in this study. (B) Body weight was monitored weekly. (C) Hematoxylin & eosin (H&E) and sirius red staining. (D) Hepatic triglycerides in liver tissue. (E) Quantitative polymerase chain reaction for mRNA expression levels of *Il1b*, *Il6*, *Mcp1*, *Tnfa*, *Acta2*, *Col1a1*, and *Tgfb*. Data are expressed as mean ± SEM (n = 6–13 per group); Chow *vs.* AMLN, *P < 0.05, **P < 0.01, ***P < 0.001; AMLN *vs.* EMPA, P < 0.05 by Student's t-test. Il1b, interleukin 1 beta; Il6, interleukin 6; Mcp1, monocyte chemoattractant protein-1; Tnfa, tumor necrosis factor alpha; Acta2, actin alpha 2; Col1a1, collagen type I alpha 1 chain; Tgfb, transforming growth factor beta; EMPA, empagliflozin; NS; not significant. (For interpretation of the references to colour in this figure legend, the reader is referred to the web version of this article.)

inhibition on NASH induces autophagy activation by suppressing SGLT2-mediated glucose overflux and subsequently decreased *O*-GlcNAcylation.

Hepatic expression and alteration of glucose transporters in NASH has not been fully investigated [31]. In hepatocytes, GLUT2 is the most abundant GLUT isoform, fulfilling the major glucose transport role [31,32]. GLUT1 also plays a role in the metabolism of hepatocytes and non-parenchymal cells in liver [32]. Changes in contributions of each GLUT family to hepatic glucose transport in several metabolic diseases including NASH are presumed [31–34]. However, the contribution of GLUT family on NAFLD remains uncertain, and even changing direction in their functional and expression status according to NAFLD has been controversial [31–36]. Thus, it is necessary to investigate whether there is another type of nutrient transporter that may additionally contribute to the onset and progression of NAFLD other than a family of GLUTs. The expression and implication of the SGLT family in the liver is not well-recognized. In this study, we decide to investigate pathophysiologic roles of SGLT2 protein in NASH liver based on the following reasons. First, SGLT2 expression is detected in primary human hepatocytes and is upregulated in liver cancer cells [37], suggesting that the expression pattern and function of hepatic SGLT2 might differ during pathogenesis of liver diseases. Increased hepatic expression of SGLT2 in NASH-related hepatocellular carcinoma mouse model further supports this hypothesis [38]. Second, we inferred a direct action of SGLT2 inhibitor on NASH liver from the previously observed benefit of SGLT2 inhibitor on NAFLD, independent of concomitant changes in weight or glycemic control, in EMPA-REG OUTCOME trial [39]. To explain independent effects of SGLT2 inhibitors on NAFLD, direct mechanism of SGLT2 inhibitor in liver was considered, but data regarding presence of SGLT2 protein in mammalian liver is controversial [40]. Thus, we tried to confirm increased expression and expanded role of hepatic SGLT2 in NASH liver using human samples and *in vitro* and *in vivo* NASH models. In humans, our study revealed higher SGLT2 expression in liver with *versus* without NASH. Further, SGLT2 expression was upregulated in hepatocytes under a NASH-mimicking *in vitro* condition. Thus, the SGLT2 contribution to glucose uptake in liver might differ according to metabolic disease status and SGLT2 inhibition might be a promising target to alleviate NASH. Increased SGLT2 expression in NASH might be attributed to activation of specific transcriptional modulators associated with nutrition-overloading in hepatocytes. For example, transcriptional modulator Specificity protein 1 (Sp-1) which is known to regulate renal SGLT2 expression [41], can be activated by nutrient (glucose) uptake and is associated with NASH pathogenesis [42–46], although such regulation in hepatocytes is not definitive.

O-GlcNAcylation, a protein posttranslational modification, is highly sensitive to nutrient availability and operates in several metabolic pathways including in the liver [13,14]. *O*-GlcNAcylation adds *O*-GlcNAc to Ser/Thr residues catalyzed by OGT and OGA removes *O*-GlcNAc from modified proteins [14]. *O*-GlcNAcylation is also controlled by the availability of its donor substrate UDP-GlcNAc synthesized by the hexosamine biosynthetic pathway (HBP) [47]. Under hyperglycemia, increased glucose flux activates HBP synthesis of UDP-GlcNAc which, in turn, causes increase in *O*-GlcNAcylated protein levels [14,48]. Not only hyperglycemia but also hyperlipidemia condition can increase *O*-GlcNAcylation levels [49]. Consistent with previous reports [48,49], we found that high-glucose and lipid conditions increased *O*-GlcNAcylation level. Based on upregulated SGLT2 expression under NASH condition in our data, we could assume that SGLT2 might serve as a transporter that mediates excessive glucose uptake and subsequently increased UDP-GlcNAc and *O*-GlcNAcylation in NASH. Similar to a recent study using 2-deoxy glucose assay [37], we showed reduced glucose uptake in hepatocytes by SGLT2 inhibition using a fluorescent analog, which may explain decrease in *O*-GlcNAcylation levels by SGLT2 modulation in this study, as observed in the kidney [50].

Protein *O*-GlcNAcylation is critical to NAFLD etiology in association with hepatic insulin resistance, lipid accumulation, inflammation, and

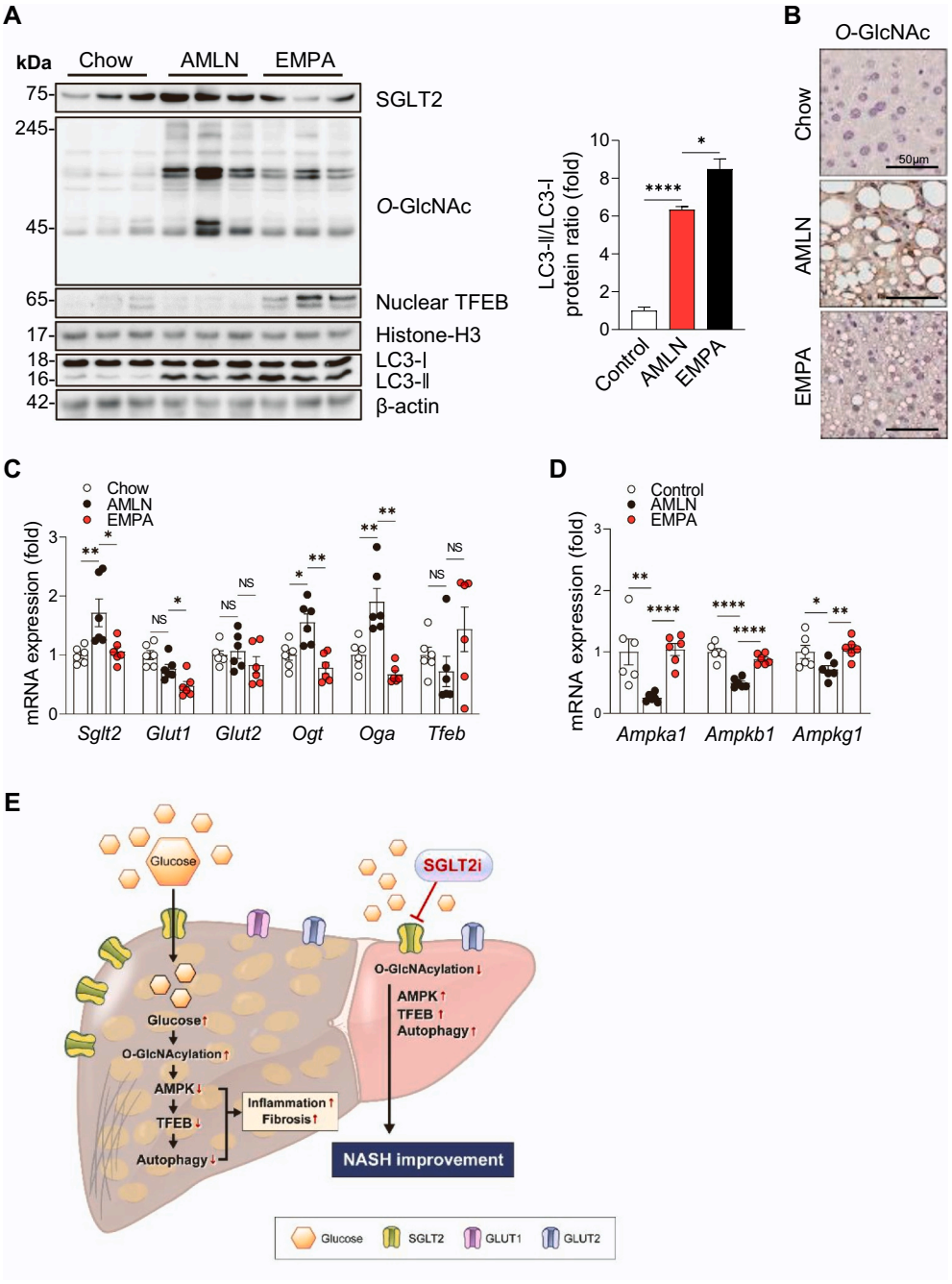

Fig. 6. The SGLT2 inhibitor reduces SGLT2 expression and *O*-GlcNAcylation with enhanced autophagic function in mice models. (A) Immunoblot analysis of SGLT2, *O*-GlcNAcylated proteins, LC3-Ⅰ/ Ⅱ, and TFEB. (B) Immunohistochemistry for *O*-GlcNAcylation expression in liver tissue. (C) Real-time qPCR for mRNA expression levels of *Sglt2*, *Glut1*, *Glut2*, *Ogt*, *Oga*, *Tfeb*, (D) *Ampka1*, *Ampkb1*, and *Ampkg1* in the liver (n = 6). (E) Summary of a novel regulatory pathway in NASH progression. Data are expressed as mean ± SEM, *P < 0.05, **P < 0.01 by Student's *t*-test. NS, not significant.

fibrosis [13,51]. The relationship between NASH and *O*-GlcNAcylation disturbance has been primarily attributed to the effect of *O*-GlcNAcylation on gluconeogenic and lipogenic transcription factors (CRTC2, FOXO1, carbohydrate response element binding protein [ChREBP], *etc.*) [13]. Autophagy is a lysosomal degradative pathway that promotes cell survival by removing damaged organelles and proteins after injury [52]. Autophagy dysfunction contributes to NAFLD variously *via* impaired degradation of intracellular lipids and exacerbated cellular injury from inflammatory cytokines [52]. However, despite the respective association of *O*-GlcNAcylation and autophagy with NASH, how aberrant *O*-GlcNAcylation affects NASH combined with autophagy dysfunction has not been sufficiently investigated.

AMPK activation is important to promote autophagic flux by increasing transcriptional activity of TFEB [10,53,54]. Recently, regulation of AMPK by *O*-GlcNAcylation was suggested, as AMPK was detected in *O*-GlcNAc precipitates and *O*-GlcNAcylation of AMPK by OGT was confirmed [55]. Increased intracellular *O*-GlcNAc inhibited AMPK activity with subsequent phosphorylation/inactivation of acetyl-CoA carboxylase in hepatocytes [49]. In bladder cancer cells, direct *O*-GlcNAcylation of AMPKα subunit downregulated its phosphorylated form and activity, thereby suppressing AMPK-mediated autophagic flux [56]. Detailed mechanism about how *O*-GlcNAcylation regulate AMPK activity in the liver needs to be further studied. In this study, increased *O*-GlcNAcylation in hepatocytes was associated with enhanced inflammation and fibrosis and suppressed AMPK activity with pathological features of insulin resistance. Inhibition or suppression of SGLT2 reduced cellular *O*-GlcNAc levels, followed by decrease in inflammation and fibrosis in association with recovery of AMPK activation, TFEB nuclear translocation, and autophagic flux in hepatocytes under NASH condition. However, the benefit of SGLT2 modulation was attenuated

when *O*-GlcNAcylation levels was reinforced by using TMG and autophagic flux was inhibited using CQ. It implies that protective effect of SGLT2 inhibition on NASH pathogenesis may be largely mediated by regulating cellular *O*-GlcNAc levels and autophagic activation. Collectively, we could infer that inhibition of upregulated hepatic SGLT2 protein in NASH liver reduces glucose overflux, leading to decrease in *O*-GlcNAcylation. Decreased *O*-GlcNAcylation recovers AMPK/TFEB-mediated autophagic activation which contributes to the amelioration of inflammation and fibrosis in NASH. In the future, the relationship between AMPK and *O*-GlcNAcylation requires further validation particularly in the NASH setting, as this relationship is complex and varies by cell type, chronic/acute stimulation, and metabolic status [55].

Our study has several limitations. First, NASH progression involves hepatocyte, macrophage, and hepatic stellate cells [57]. However, the effect of SGLT2 inhibition was only examined in hepatocytes as we did not observe increased SGLT2 expression in other cell types. Further studies should evaluate SGLT2 inhibition in NASH in the context of cell-cell interaction among macrophages and hepatic stellate cells as well. Second, the relative contributions of GLUT family and SGLT2 in glucose uptake under NASH conditions has not been investigated. Any potential compensatory increase in GLUT activity by SGLT2 inhibition and utility of a dual antagonist against SGLT2 and GLUT family for NASH treatment needs further study. As data about glucose transporters in human NASH are insufficient, their expression patterns need further investigation.

5. Conclusion

To the best of our knowledge, this study is the first to provide evidence that SGLT2 protein is significantly increased in human NASH liver and its inhibition ameliorates NASH *via* reduced *O*-GlcNAcylation with subsequent autophagy activation. Further investigation is needed to elucidate whether SGLT2-mediated hepatic glucose uptake effectively modulates glucose overload-mediated aberrant *O*-GlcNAcylation and autophagy suppression in NASH.

Supplementary data to this article can be found online at https://doi.org/10.1016/j.metabol.2023.155612.

Funding sources

This research was supported by National Research Foundation of Korea (NRF) Grant funded by the Korean Government (MSIP) (No. Grant Number: NRF-2016R1A5A1010764 and NRF-2019R1l1A1A01063695) and by Basic Science Research Program through the NRF funded by the Ministry of Education (2018R1D1A1B07050005 and NRF-2021R1I1A1A01048435) and by the KHIDI-AZ Diabetes Research Program. Funding agencies did not affect the collection, analysis, or presentation of the data.

CRediT authorship contribution statement

H.J.C., E.R.K., and M.L. carried out experiments and analyzed the data. E.R.K. and M.L. wrote the manuscript, and H.J.C., E.R.K., and M.L. performed the statistical analysis. D.H.C., S.H.K., and E.S. contributed to acquisition of data. J-H.K., J.W.C., and D.H.H. provided advice and consultation throughout. D.H.H., B-S.C., and Y-h.L. contributed to the conception and design of the study, the interpretation of data, and the drafting of the manuscript. Y-h.L. is the guarantor of this work and, as such, had full access to all the data in the study and takes responsibility for the integrity of the data and the accuracy of the data analysis.

Declaration of competing interest

Yong-ho Lee consults for Panolos Bioscience and owns stock in Panolos Bioscience. Declarations of interest for other authors: none.

Acknowledgements

Caron Modeas, Evolved Editing, LLC, provided editorial assistance. She had no role in the study design, implementation, or analysis. The authors thank Medical Illustration & Design(MID), a part of the Medical Research Support Services of Yonsei University College of Medicine, for providing excellent support with medical illustration.

References

[1] Cotter TG, Rinella M. Nonalcoholic fatty liver disease 2020: the state of the disease. Gastroenterology 2020;158:1851–64.
[2] Chalasani N, Younossi Z, Lavine JE, Charlton M, Cusi K, Rinella M, et al. The diagnosis and management of nonalcoholic fatty liver disease: practice guidance from the American Association for the Study of Liver Diseases. Hepatology 2018; 67:328–57.
[3] Eslam M, Newsome PN, Sarin SK, Anstee QM, Targher G, Romero-Gomez M, et al. A new definition for metabolic dysfunction-associated fatty liver disease: an international expert consensus statement. J Hepatol 2020;73:202–9.
[4] Kim K-S, Hong S, Ahn H-Y, Park C-Y. Metabolic dysfunction-associated fatty liver disease and mortality: a population-based cohort study. Diabetes Metab J 2023;47: 220–31.
[5] Lee BW, Lee YH, Park CY, Rhee EJ, Lee WY, Kim NH, et al. Non-alcoholic fatty liver disease in patients with type 2 diabetes mellitus: a position statement of the fatty liver research Group of the Korean Diabetes Association. Diabetes Metab J 2020; 44:382–401.
[6] Jeong SW. Nonalcoholic fatty liver disease: a drug revolution is coming. Diabetes Metab J 2020;44:640–57.
[7] Kaneto H, Obata A, Kimura T, Shimoda M, Kinoshita T, Matsuoka TA, et al. Unexpected pleiotropic effects of SGLT2 inhibitors: pearls and pitfalls of this novel antidiabetic class. Int J Mol Sci 2021;22.
[8] Sheu WHH, Chan SP, Matawaran BJ, Deerochanawong C, Mithal A, Chan J, et al. Use of SGLT-2 inhibitors in patients with type 2 diabetes mellitus and abdominal obesity: an Asian perspective and expert recommendations. Diabetes Metab J 2020; 44:11–32.
[9] Kim NH, Kim NH. Renoprotective mechanism of sodium-glucose cotransporter 2 inhibitors: focusing on renal hemodynamics. Diabetes Metab J 2022;46:543–51.
[10] Kim SH, Kim G, Han DH, Lee M, Kim I, Kim B, et al. Ezetimibe ameliorates steatohepatitis via AMP activated protein kinase-TFEB-mediated activation of autophagy and NLRP3 inflammasome inhibition. Autophagy 2017;13:1767–81.
[11] Mu W, Cheng X-F, Liu Y, Lv Q-Z, Liu G-L, Zhang J-G, et al. Potential Nexus of non-alcoholic fatty liver disease and type 2 diabetes mellitus: insulin resistance between hepatic and peripheral tissues. Front Pharmacol 2019;9:1566.
[12] Alnahdi A, John A, Raza H. Augmentation of glucotoxicity, oxidative stress, apoptosis and mitochondrial dysfunction in HepG2 cells by palmitic acid. Nutrients 2019;11.
[13] Zhang K, Yin R, Yang X. O-GlcNAc: a bittersweet switch in liver. Front Endocrinol 2014;5:221.
[14] Mueller T, Ouyang X, Johnson MS, Qian W-J, Chatham JC, Darley-Usmar V, et al. New insights into the biology of protein O-GlcNAcylation: approaches and observations. Frontiers Aging 2021:1.
[15] Fukushima K, Kitamura S, Tsuji K, Wada J. Sodium–glucose cotransporter 2 inhibitors work as a "regulator" of autophagic activity in overnutrition diseases. Front Pharmacol 2021;12.
[16] Obara K, Shirakami Y, Maruta A, Ideta T, Miyazaki T, Kochi T, et al. Preventive effects of the sodium glucose cotransporter 2 inhibitor tofogliflozin on diethylnitrosamine-induced liver tumorigenesis in obese and diabetic mice. Oncotarget 2017;8:58353–63.
[17] Kleiner DE, Makhlouf HR. Histology of nonalcoholic fatty liver disease and nonalcoholic steatohepatitis in adults and children. Clin Liver Dis 2016;20: 293–312.
[18] Kleiner DE, Brunt EM, Van Natta M, Behling C, Contos MJ, Cummings OW, et al. Design and validation of a histological scoring system for nonalcoholic fatty liver disease. Hepatology 2005;41:1313–21.
[19] Jensen T, Abdelmalek MF, Sullivan S, Nadeau KJ, Green M, Roncal C, et al. Fructose and sugar: a major mediator of non-alcoholic fatty liver disease. J Hepatol 2018;68:1063–75.
[20] Trevaskis JL, Griffin PS, Wittmer C, Neuschwander-Tetri BA, Brunt EM, Dolman CS, et al. Glucagon-like peptide-1 receptor agonism improves metabolic, biochemical, and histopathological indices of nonalcoholic steatohepatitis in mice. Am J Physiol Gastrointest Liver Physiol 2012;302:G762–72.
[21] Koppe SW, Elias M, Moseley RH, Green RM. Trans fat feeding results in higher serum alanine aminotransferase and increased insulin resistance compared with a standard murine high-fat diet. Am J Physiol Gastrointest Liver Physiol 2009;297: G378–84.
[22] Kim Y, Lee SW, Wang H, Kim R-H, Park HK, Lee H, et al. DA-1241, a novel GPR119 agonist, improves Hyperglycaemia by inhibiting hepatic gluconeogenesis and enhancing insulin secretion in diabetic mice. Diabetes Metab J 2022;46:337–48.
[23] Lee YH, Cho Y, Lee BW, Park CY, Lee DH, Cha BS, et al. Nonalcoholic fatty liver disease in diabetes. Part I: epidemiology and diagnosis. Diabetes Metab J 2019;43: 31–45.
[24] Müller FA, Sturla SJ. Human in vitro models of nonalcoholic fatty liver disease. Curr Opin Toxicol 2019;16:9–16.

[25] Cui W, Chen SL, Hu KQ. Quantification and mechanisms of oleic acid-induced steatosis in HepG2 cells. Am J Transl Res 2010;2:95–104.
[26] Ding WJ, Wu WJ, Chen YW, Chen HB, Fan JG, Qiao L. Expression of Notch family is altered in non-alcoholic fatty liver disease. Mol Med Rep 2020;22:1702–8.
[27] Kwan HY, Niu X, Dai W, Tong T, Chao X, Su T, et al. Lipidomic-based investigation into the regulatory effect of Schisandrin B on palmitic acid level in non-alcoholic steatotic livers. Sci Rep 2015;5:1–14.
[28] Zhang X, Qiao Y, Wu Q, Chen Y, Zou S, Liu X, et al. The essential role of YAP O-GlcNAcylation in high-glucose-stimulated liver tumorigenesis. Nat Commun 2017;8:1–15.
[29] Housley MP, Rodgers JT, Udeshi ND, Kelly TJ, Shabanowitz J, Hunt DF, et al. O-GlcNAc regulates FoxO activation in response to glucose. J Biol Chem 2008;283:16283–92.
[30] Long YC, Zierath JR. AMP-activated protein kinase signaling in metabolic regulation. J Clin Invest 2006;116:1776–83.
[31] Karim S, Adams DH, Lalor PF. Hepatic expression and cellular distribution of the glucose transporter family. World J Gastroenterol 2012;18:6771–81.
[32] Chadt A, Al-Hasani H. Glucose transporters in adipose tissue, liver, and skeletal muscle in metabolic health and disease. Pflugers Arch 2020;472:1273–98.
[33] Karim S, Liaskou E, Fear J, Garg A, Reynolds G, Claridge L, et al. Dysregulated hepatic expression of glucose transporters in chronic disease: contribution of semicarbazide-sensitive amine oxidase to hepatic glucose uptake. Am J Physiol Gastrointest Liver Physiol 2014;307:G1180–90.
[34] Okamoto Y, Tanaka S, Haga Y. Enhanced GLUT2 gene expression in an oleic acid-induced in vitro fatty liver model. Hepatol Res 2002;23:138–44.
[35] Rubio A, Guruceaga E, Vázquez-Chantada M, Sandoval J, Martínez-Cruz LA, Segura V, et al. Identification of a gene-pathway associated with non-alcoholic steatohepatitis. J Hepatol 2007;46:708–18.
[36] Li X, Li J, Lu X, Ma H, Shi H, Li H, et al. Treatment with PPARδ agonist alleviates non-alcoholic fatty liver disease by modulating glucose and fatty acid metabolic enzymes in a rat model. Int J Mol Med 2015;36:767–75.
[37] Kaji K, Nishimura N, Seki K, Sato S, Saikawa S, Nakanishi K, et al. Sodium glucose cotransporter 2 inhibitor canagliflozin attenuates liver cancer cell growth and angiogenic activity by inhibiting glucose uptake. Int J Cancer 2018;142:1712–22.
[38] Jojima T, Wakamatsu S, Kase M, Iijima T, Maejima Y, Shimomura K, et al. The SGLT2 inhibitor canagliflozin prevents carcinogenesis in a mouse model of diabetes and non-alcoholic steatohepatitis-related hepatocarcinogenesis: association with SGLT2 expression in hepatocellular carcinoma. Int J Mol Sci 2019;20:5237.
[39] Sattar N, Fitchett D, Hantel S, George JT, Zinman B. Empagliflozin is associated with improvements in liver enzymes potentially consistent with reductions in liver fat: results from randomised trials including the EMPA-REG OUTCOME(R) trial. Diabetologia 2018;61:2155–63.
[40] Aschenbach JR, Steglich K, Gabel G, Honscha KU. Expression of mRNA for glucose transport proteins in jejunum, liver, kidney and skeletal muscle of pigs. J Physiol Biochem 2009;65:251–66.
[41] Zhao Y, Gao P, Sun F, Li Q, Chen J, Yu H, et al. Sodium intake regulates glucose homeostasis through the PPAR delta/adiponectin-mediated SGLT2 pathway. Cell Metab 2016;23:699–711.
[42] Comer FI, Hart GW. O-GlcNAc and the control of gene expression. BBA Gen Subjects 1999;1473:161–71.
[43] Yamamoto T, Watanabe K, Inoue N, Nakagawa Y, Ishigaki N, Matsuzaka T, et al. Protein kinase Cbeta mediates hepatic induction of sterol-regulatory element binding protein-1c by insulin. J Lipid Res 2010;51:1859–70.
[44] Charlton M, Krishnan A, Viker K, Sanderson S, Cazanave S, McConico A, et al. Fast food diet mouse: novel small animal model of NASH with ballooning, progressive fibrosis, and high physiological fidelity to the human condition. Am J Physiol Gastrointest Liver Physiol 2011;301:G825–34.
[45] Chen S, Li H, Zhang J, Jiang S, Zhang M, Xu Y, et al. Identification of Sp1 as a transcription activator to regulate fibroblast growth factor 21 gene expression. Biomed Res Int 2017;2017:8402035.
[46] Seo H-Y, Kim M-K, Jung Y-A, Jang BK, Yoo E-K, Park K-G, et al. Clusterin decreases hepatic SREBP-1c expression and lipid accumulation. Endocrinology 2013;154:1722–30.
[47] Liu Y, Yao RZ, Lian S, Liu P, Hu YJ, Shi HZ, et al. O-GlcNAcylation: the “stress and nutrition receptor” in cell stress response. Cell Stress Chaperones 2021;26:297–309.
[48] Butkinaree C, Park K, Hart GW. O-linked beta-N-acetylglucosamine (O-GlcNAc): extensive crosstalk with phosphorylation to regulate signaling and transcription in response to nutrients and stress. Biochim Biophys Acta 2010;1800:96–106.
[49] Pang Y, Xu X, Xiang X, Li Y, Zhao Z, Li J, et al. High fat activates O-GlcNAcylation and affects AMPK/ACC pathway to regulate lipid metabolism. Nutrients 2021;13.
[50] Otomo H, Nara M, Kato S, Shimizu T, Suganuma Y, Sato T, et al. Sodium-glucose cotransporter 2 inhibition attenuates protein overload in renal proximal tubule via suppression of megalin O-GlcNacylation in progressive diabetic nephropathy. Metab Clin Experiment 2020:113.
[51] Zhou Y, Li Z, Xu M, Zhang D, Ling J, Yu P, et al. O-GlycNacylation remission retards the progression of non-alcoholic fatty liver disease. Cells 2022;11:3637.
[52] Czaja MJ. Function of autophagy in nonalcoholic fatty liver disease. Dig Dis Sci 2016;61:1304–13.
[53] Napolitano G, Esposito A, Choi H, Matarese M, Benedetti V, Di Malta C, et al. mTOR-dependent phosphorylation controls TFEB nuclear export. Nat Commun 2018;9:3312.
[54] Paquette M, El-Houjeiri L, Zirden LC, Puustinen P, Blanchette P, Jeong H, et al. AMPK-dependent phosphorylation is required for transcriptional activation of TFEB and TFE3. Autophagy 2021;17:3957–75.
[55] Gelinas R, Dontaine J, Horman S, Beauloye C, Bultot L, Bertrand L. AMP-activated protein kinase and O-GlcNAcylation, two partners tightly connected to regulate key cellular processes. Front Endocrinol (Lausanne) 2018;9:519.
[56] Jin L, Yuan F, Dai G, Yao Q, Xiang H, Wang L, et al. Blockage of O-linked GlcNAcylation induces AMPK-dependent autophagy in bladder cancer cells. Cell Mol Biol Lett 2020;25:1–13.
[57] Lefere S, Puengel T, Hundertmark J, Penners C, Frank AK, Guillot A, et al. Differential effects of selective- and pan-PPAR agonists on experimental steatohepatitis and hepatic macrophages. J Hepatol 2020;73:757–70.